

FIELD-DEPENDENT SURFACE RESISTANCE FOR SUPERCONDUCTING NIOBIUM ACCELERATING CAVITIES: THE CASE OF N-DOPING

W. Weingarten, visiting fellow at Cornell University*

R. Eichhorn, Cornell Laboratory for Accelerator-Based Sciences and Education, Ithaca, NY, USA

Abstract

The dependence of the Q-value on the RF field (Q-slope) for superconducting RF cavities is actively studied in various accelerator laboratories. Although remedies against this dependence have been found, the physical cause still remains obscure. A rather straightforward two-fluid model description of the Q-slope in the low and high field domains is extended to the case of the experimentally identified increase of the Q-value with the RF field obtained by so-called "N-doping".

INTRODUCTION

So-called "N-doped" niobium superconducting (sc) cavities obtained increased interest, because they hold the promise of large Q-values at technically still useful accelerating gradients. They exhibit an increase of the Q-value below 2.1-2.5 K with the RF magnetic surface field B (negative Q-slope) up to about 60-80 mT, equivalent to 15-20 MV/m accelerating gradient. This observation was repeatedly observed in different laboratories [1, 2, 3]. A typical data set is shown in Fig. 1.

It shows the Q-value vs the magnetic surface field B of a 1.3 GHz single cell cavity, made of bulk niobium and fired in a N₂ atmosphere [p=50 mTorr (66 hPa), 800°C, 20 minutes], electro-polished, prepared at FNAL and tested at Cornell at different temperatures (from top to bottom, 1.6, 1.7, 1.8, 1.9, 2.0, 2.1, 2.5, 3.0 and 4.2 K) [4]. For an accelerating gradient of 10 MV/m the surface magnetic field B amounts to 42 mT. The continuous lines result from the fit to the data with $Q=270.7 \Omega/R_s$, with R_s described by eq. 4. The maximum gradient was limited by a quench.

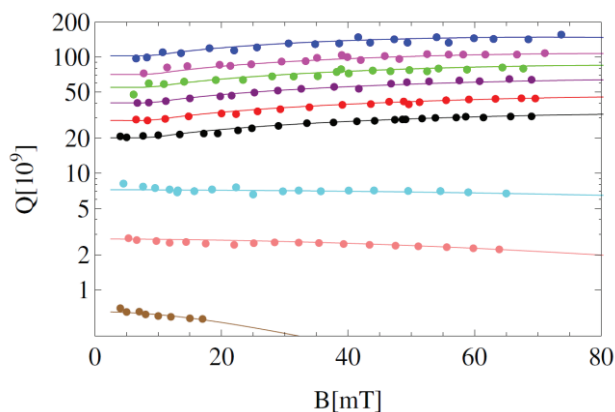


Figure 1: Q vs. B curve of 1.3 GHz N-doped cavity.

* wolfgang.weingarten@cern.ch

Accelerating cavities treated by N-doping are not free from the previously observed decrease of the Q-value with the RF magnetic field (Q-slope and Q-drop). These observations were described in several models [5, 6, 7, 8], but a unanimously accepted explanation is missing. Recipes to improve cavity performance were nevertheless found [5]. The present paper presents a data analysis of the experimental results as of Fig. 1 and presents a common description of the observed Q-increase and Q-decrease.

Our paper is organized as such. In a first step we present the model as of ref. 6 for weak sc defects at the surface caused by oxygen. Then we extend the model for similar defects in the bulk made up of nitrogen. Secondly, by a zero level analysis, we identify the important variables describing the data (Table 1). "Zero level" alludes to using Microsoft EXCEL® as fitting tool. We then use the MATHEMATICA® software for fitting the data related to the N-doped cavity of Fig. 1, discuss the results, and draw a conclusion.

DESCRIPTION OF MODEL

RF Magnetic Field Dependence of Weak SC Defects

Our analysis is based on the two-fluid model of RF superconductivity with emphasis on the electrical conductivity of the nc component of the superconductor.

For a **weak sc defect located at the surface**, we apply the model as outlined in ref. 6, however no longer for the specific case of an Nb/NbO composite but instead for an Nb/NbN composite. This model states that the surface layer is non-uniform in terms of having defects being only weak superconductors. The defect has mesoscopic size, embedded in the sc "host" metal of high purity and in close contact with this. The weak sc defect would be nc if not in the vicinity of a sc host metal. The defect is supposed to have sc properties induced from, and weaker than, the sc "host" metal Nb (Cooper pairs, characteristic coherence length ξ_N , lower critical field B_c^* and lower critical temperature than the sc host metal). The defect also induces normal-conducting (nc) charge carriers into the otherwise sc host metal. All these features are typical of the sc proximity-effect.

The model states the entry of magnetic flux above relatively small magnetic fields and an increase of the Q-slope above the "surface percolation temperature" T^* , which is typically in the order of 2.1 K (for an Nb/NbO composite). Energy balance considerations lead to the following results. The magnetic field B_c^* for the first entry of magnetic flux at the weak sc defect as nucleation centre,

$$B_c^* \approx \frac{B_c}{\kappa^{3/2}},$$

may become much smaller than the thermodynamic critical field B_c , because the local coherence length ξ close to the surface may become pretty small and the local penetration depth λ at the surface rather large. For a mean free path $L=10$ nm, for example, one finds, for niobium, $\xi=8$ nm, $\lambda=83$ nm and $B_c^*=6$ mT (with $B_c=200$ mT). The additional field dependent surface resistance R_s' originating from the defects at the surface is

$$R_s' = \{R_{s1} + R_{s2} \cdot \Theta(T - T^*) \cdot (T - T^*)^\beta\} \cdot (-\kappa^{-2}) \left\{ 1 + \frac{\ln\left[1 - \left(\frac{\kappa B}{B_c}\right)^2\right]}{\left(\frac{\kappa B}{B_c}\right)^2} \right\}. \quad (1)$$

Here the surface resistances R_{s1} and R_{s2} account for the entry of magnetic flux at the surface below and above the percolation temperature, respectively. The increase of the weak sc defect density above T^* is described by the Heaviside Θ -function and is governed by the phenomenological exponent β . κ is the Ginzburg-Landau parameter of niobium (~ 1). Eq. 1 describes the medium field Q-slope and, by force of the singularity at $B=B_c/\kappa$, the high field Q-drop as well.

In ref. 6 the weak sc defects were made up, as a showcase, by a composite of a strong superconductor (Nb) and a normal conductor in its proximity (NbO above 1.4 K).

For a **weak sc defect in the bulk** we apply a slightly modified approach as of ref. 6, this time for an Nb/NbN composite.

The data of an N-doped cavity (Fig. 1) allow describing how deep-lying weak sc defects located in the bulk will react to the RF magnetic field B . The SIMS elemental depth profile [4] shows large excess nitrogen at the surface and less down into the bulk (Fig. 2). The N-doped cavities show best performance after chemical removal of several μm of niobium. Fig. 2 teaches us that thereafter the N depth profile is pretty constant.

For the weak sc defect in the bulk, and contrary to the one at the surface, when exposed to the RF magnetic field B , there is no gain in diamagnetic volume energy with increasing B , when the critical magnetic field B_c^* of the defect is surpassed. The reason is that, contrary to the situation at the surface, the RF current diverts symmetrically around the defect, when in the nc state.

However, the weak sc defect in the bulk is also subject to the sc proximity effect, being in the sc state thanks the proximity of a strong superconductor for sufficiently low magnetic fields, otherwise being nc.

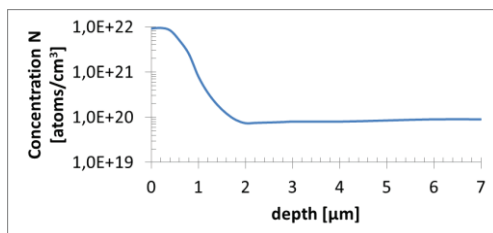


Figure 2: Nitrogen depth profile.

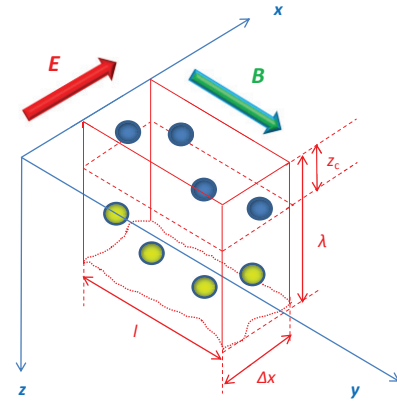


Figure 3: Surface element with weak sc defects.

Fig. 3 depicts a current-carrying element inside the sc metal. The current flows in x-direction, the magnetic and electric fields B and E decay exponentially deeper inside the metal with the characteristic decay length (the sc penetration depth λ). Minute weak sc defects are symbolized by coloured spheres. The defects which have not yet transitioned into the nc state are coloured green; those which have are coloured blue. A characteristic depth $z_c(B)$ depends on the surface magnetic field B and discriminates the upper part, where the defects are nc, against the lower one, where they are sc.

If B is increased, those weak sc defects located within the distance z_c , for which B inside the metal $B_z = B \cdot \exp(z/\lambda)$ exceeds B_c^* , are nc. The distance z_c of weak sc defects having already transitioned into the nc state increases therefore with B according to $z_c(B) = \lambda \cdot \ln(B/B_c^*)$. So does the volume fraction $f(B)$ of the weak sc defects when in the nc state. The provision is made that the density of the weak sc defects is uniform with depth z . This is, according to Fig. 2, fairly well correct after removal of the surface layer by electro-polishing.

In what follows we derive the sc surface resistance R_s of a slab as depicted in Fig. 3. For convenience we apply the lumped circuit model description of current flow. The power dissipation ΔP inside the slab of width Δx , cross section $\lambda \cdot l$, and resistance R is

$$\Delta P = V^2 / (2R).$$

V is the voltage across this slab, which is created by the Meissner current at the surface, or, equivalently, the RF surface magnetic field B ,

$$V = -i\omega\lambda B \cdot \Delta x.$$

As the same voltage V is acting on both the sc and nc electrons, the resistance R is composed in parallel circuit arrangement of the resistances R_1 and R_2 ,

$$1/R = 1/R_1 + 1/R_2.$$

R_1 is associated with the super-current's nc component and R_2 is associated with the current across the weak sc defects, when they are nc. The corresponding electrical conductivities are σ_1 and σ_2 with the associated mean free paths L_1 and L_2 , respectively,

$$\sigma_{1,2}(T) = \frac{n(T)e^2 L_{1,2}}{m v_F}. \quad (2)$$

$n(T)$ is the density of the nc electrons, depending on T , e their electric charge, m their effective mass and v_F their Fermi velocity.

Now we assume that weak sc defects of size small compared to the sc penetration depth λ are located inside a surface layer (symbolized in Fig. 3 by the blue and green little spheres). As outlined before, the volume fraction f of weak sc defects that already have become nc is zero for $B \leq B_c^*$ and increases for $B > B_c^*$ up till B_c , at the utmost, as

$$f(B) = \begin{cases} \ln(B/B_c^*)/\ln(B_c/B_c^*), & B \geq B_c^* \\ 0, & \text{else} \end{cases}$$

with $f(B_c) = 1$. With the symbols as shown in Fig. 3 the respective resistances are

$$1/R_1 = (\lambda/\Delta x) \cdot \sigma_1(T) \cdot [1 - f(B)]$$

and

$$1/R_2 = (\lambda/\Delta x) \cdot \sigma_2(T) \cdot f(B).$$

Substituting and rearranging terms, we get with $B = -\mu_0 \cdot H$,

$$\Delta P = (1/2)\omega^2 \lambda^2 \mu_0^2 H^2 \cdot \lambda \cdot \{\sigma_1(T)[1 - f(B)] + \sigma_2(T)f(B)\} \cdot \Delta x.$$

Therefore the electrical conductivity σ , averaged over the volume, is composed of a sum. Its first component is governed by the electrical conductivity $\sigma_1(T)$ or, equivalently, the mean free path L_1 , of the nc current component when all defects are in the sc state ($f(B)=0$). Its second component is determined by the electrical conductivity $\sigma_2(T)$ or, equivalently, the mean free path L_2 , of the nc current component when all defects are in the nc state ($f(B)=1$). The sharing between these two states is determined by the magnetic RF field B via $f(B)$:

$$\sigma(T, B) \sim \sigma_1(T) \cdot [1 - f(B)] + \sigma_2(T) \cdot f(B).$$

The dissipated power per unit-square is $p = \Delta P / (\lambda \cdot \Delta x)$, from which the surface resistance $R_s = 2 \cdot p / H^2$ can be derived,

$$R_s = \overbrace{\omega^2 \lambda^3 \mu_0^2 \{\sigma_1(T)\} [1 - f(B)] + \sigma_2(T) f(B)}^{R_{s,BCS}} = R_{s,BCS} \cdot \{[1 - f(B)] + (\sigma_2(T)/\sigma_1(T))f(B)\}. \quad (3)$$

However, we know that for $B \leq B_c^*$, when $f(B)=0$, the surface resistance R_s is composed of the BCS surface resistance $R_{s,BCS}$ and the residual surface resistance R_{res} , which we consequently have to add to $R_{s,BCS}$.

Temperature Dependence of Weak SC Defects

The proximity between the nc and sc metal induces nc charge carriers into the latter, thus increasing the normal

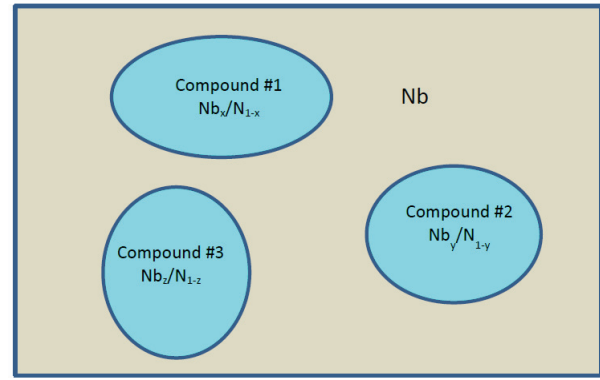


Figure 4: Compounds of weak sc defects inside composite.

state conductivity of the sc metal. By percolation above T^* the nc metal is fragmented with increasing temperature into smaller pieces separated by long range sc paths. Hence this fragmentation enlarges the proximity interface between nc and sc metal as well as the mean free path of the nc electrons and hence increases the normal state conductivity of the sc metal.

We call the weak sc defect composed of nitrogen dissolved in niobium (Nb_x/N_{1-x}) of still unspecified and variable atomic compositions x , y or z of Nb a “compound”. We call these compounds, if embedded in a niobium matrix, a “composite”, as visualized in Fig. 4. If the composite is located at the surface, the nc volume will increase and is subject to the percolation action above T^* . The related field dependent surface resistance is described by eq. 1.

If the weak sc defect is located in the bulk, the conductivity will increase stepwise above the “bulk percolation temperature” T'^* , possibly different from T^* , to a constant value, as suggested by the constant N-depth profile, Fig. 2. We call the related electrical conductivity σ_{bulk} , being proportional to

$$\sigma_{bulk}(T, B) \sim \sigma_1(T) \cdot [1 - f(B)] + \sigma_2(T) \cdot f(B)$$

with, using eq. 2,

$$\sigma_2(T) = \sigma_1(T) \cdot [L_2/L_1 + \Theta(T - T'^*) \cdot \Delta(L_2/L_1)].$$

Hence, the total surface resistance is composed of the contributions as in eqs. 1 and 3, including the addition of R_{res} , as explained before. The stepwise increase of R_s at the percolation thresholds T^* and T'^* have to be added as well, yielding:

$$R_s = \left(A \cdot \frac{e^{-\Delta/T}}{T} + R_{res} \right) \cdot \{1 - f(B) + f(B) \cdot [L_2/L_1 + \Theta(T - T'^*) \cdot \Delta(L_2/L_1)]\} + \{R_{s1} + R_{s2} \cdot \Theta(T - T^*) \cdot (T - T^*)^\beta\} \cdot (-\kappa^{-2}) \cdot \left\{ 1 + \frac{\ln\left[1 - \left(\frac{\kappa B}{B_c}\right)^2\right]}{\left(\frac{\kappa B}{B_c}\right)^2} \right\}. \quad (4)$$

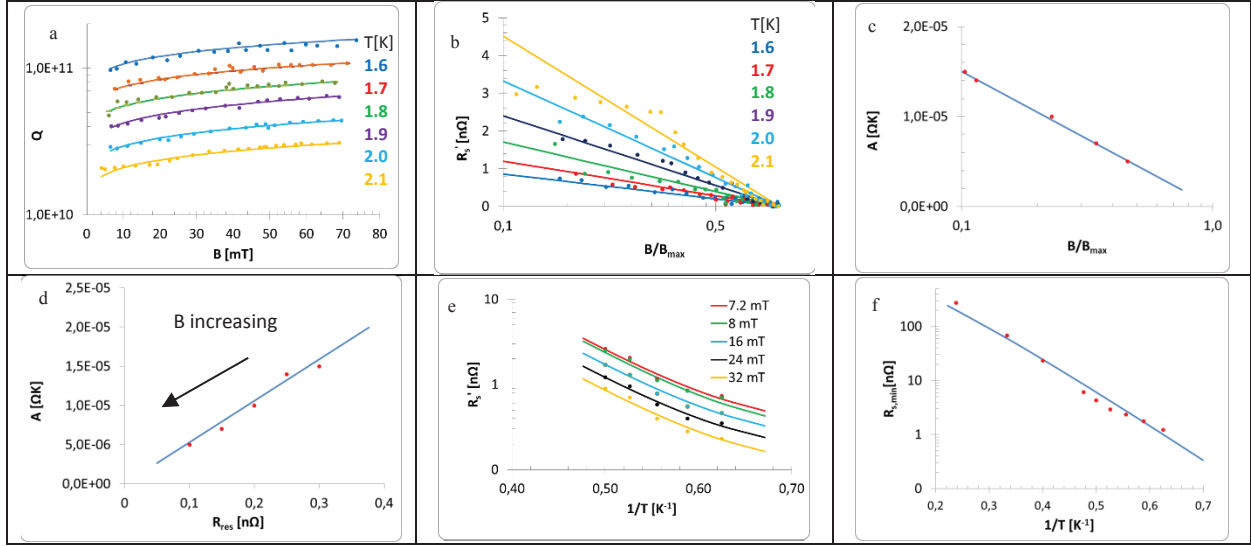
ANALYSIS OF DATA AND DISCUSSION

Zero Level Data Analysis

In Table 1 we restrict ourselves for the moment on the temperature range for which Q increases with field ($T \leq 2.1$ K). The following parameters are plotted. The surface resistance $R_s(T, B)$ is separated into a non-field-dependent

part $R_{s,BCS} + R_{res}$ and a field- and temperature-dependent part R_s' . $R_{s,BCS}$ is the temperature dependent BCS surface resistance and R_{res} is the temperature independent residual surface resistance, resulting in $R_s(T, B) = R_{s,BCS}(T) + R_{res} + R_s'(T, B)$. The BCS surface resistance is parametrised as $R_{s,BCS} = (A/T) \cdot \exp(-\Delta/T)$, A

Table 1: Zero-level analysis



being a constant depending on the material and frequency, Δ the sc energy gap and T the temperature. B is the surface RF magnetic field near the equator of the cavity and vicinity and B_{\max} is the maximum experimentally obtained magnetic field there before the cavity quenched.

Inspecting the data of Table 1 allows drawing the following propositions:

1. as deduced from d) and e): a field dependent penetration depth λ or a field dependent energy gap Δ provide no basis to explain R_s' as measured;
2. as deduced from a): The Q-value factorizes into a temperature and a field dependent part as $Q \sim g(T) \cdot h(B)$;
3. as deduced from b): The field dependent part of R_s' depends on B as $R_s' \sim \text{const} \cdot \ln(B)$;
4. as deduced from e): The temperature dependent part of R_s' depends on T as $R_s' \sim R_{s,BCS}(T) + R_{\text{res}}$;
5. as deduced from f): The minimum residual surface resistance R_{res} (obtained at about B_{\max}) continues decreasing below 1 nΩ without any sign of saturation.

These propositions are indeed confirmed by eq. 4.

Data Fitting

We use the MATHEMATICA® package to find the best fit by χ^2 -minimization for the parameters as of eq. 4, this time for the whole temperature range from 1.6 to 4.2 K (Table 2).

The a priori well known parameters A , Δ , and R_{res} were left free as “witness” fit parameters, whereas B_c and κ were fixed parameters. The relative error for the measurement of the surface resistance of $\pm 4\%$ results in $\chi^2=122$, close enough to the number of data points (167), reduced by the number of fit parameters (11). Most of the fit parameters are uncorrelated and the χ^2 -function displays an inverse bell-shaped minimum. The correlated ones are either factors in a product or tied by a common B- or T-dependence, for which the correlation is understandable. We take as error of the fit parameters the

one where the χ^2 -value is twice its minimum value with all other fit parameters kept at their χ^2 -minimum value.

Table 2: Result of Least-Square Fitting

Fit Parameter	Fitted value	Unit
A	$(119 \pm 5) \cdot 10^3$	nΩ·K
Δ	17.9 ± 0.1	K
R_{res}	2.0 ± 0.2	nΩ
β	$7.5 \pm \frac{1}{5}$	-
R_{s1}	3.4 ± 4.0	nΩ
R_{s2}	3.6 ± 3.0	nΩ
L_2/L_1	0.40 ± 0.06	-
$\Delta(L_2/L_1)$	0.6 ± 0.2	-
T^*	$1.1 \pm \frac{1.2}{0.2}$	K
T^{*2}	2.3 ± 0.2	K
B_c^*	9.0 ± 2.5	mT
Fix Parameter	Non-fitted value	Unit
B_c	200	mT
κ	1	-

Consistency Check

From the literature we know that the lowest critical temperature of the $\text{Nb}_x/\text{N}_{1-x}$ compound is 1.2 K [9], close to the fitted values. The equivalent volume fraction is 15 atomic percent of nitrogen in niobium (as obtained for a thin film in the cubic W-phase), hence $x=0.85$.

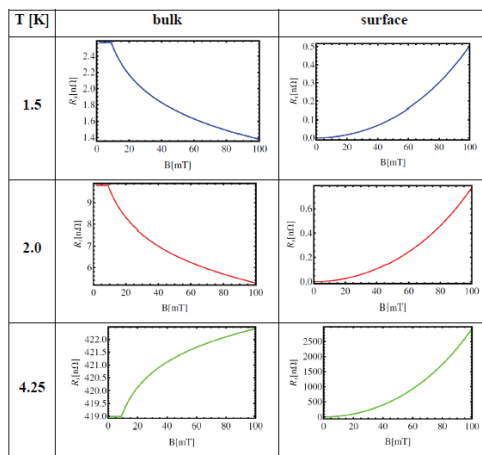
We check now the consistency of this number with the SIMS depth profile of the nitrogen content (Fig. 2). With Avogadro's number ($N_A=6 \cdot 10^{23} \text{ Mol}^{-1}$), the atomic number of Nb ($A=93$), its density ($\rho=8.6 \text{ g} \cdot \text{cm}^{-3}$), the atomic density of N-atoms at the surface is $5.5 \cdot 10^{22} \text{ cm}^{-3}$. For the relative composition N/Nb of the compound of 15 %, this number corresponds to an atomic density of N-atoms at the surface $0.83 \cdot 10^{22} \text{ cm}^{-3}$, very close to what was found at the surface before removal of the uppermost layers by electro-polishing. Hence we conclude that, after electro-polishing, when the nitrogen volume density,

$0.8 \cdot 10^{20}$ nitrogen atoms per cm^3 , is lower by a factor of 100, as we learn from the SIMS depth profile, surface defects are still present, however dispersed by this same factor. We also estimated the size of the compound inside the bulk from the Ginzburg-Landau parameter $\kappa \approx 1$, being amidst its χ^2 error interval. The corresponding mean free path is 450 nm, with the London penetration depth $\lambda_L = 29$ nm and the intrinsic coherence length $\xi_0 = 33$ nm. If the mean free path is determined by interstitially arranged nitrogen atoms, the nitrogen atomic volume density is 10^{13} atoms $\cdot \text{cm}^{-3}$. As the measured atomic nitrogen density is larger by a factor 10^7 , the $\text{Nb}_x/\text{N}_{1-x}$ compound must have a linear dimension of about 215 atoms or 56 nm as upper limit.

Considerations for Accelerator Operation

Table 3 shows the contributions, at different temperatures, of the field dependent surface resistance R_s' to the total surface resistance for weak sc defects in the bulk and at the surface defects, respectively. When inspecting Table 3, the worst case, from an operational point of view, is clearly identified as 4.25 K and in presence of a large number of surface weak sc defects (mind the scales!). On the contrary, the optimum case is at a temperature smaller than T^* (~ 2.3 K). The models shows that for surface defects there is always a tendency for an increase of the field dependent surface resistance at all temperatures.

Table 3: Contributions to R_s' from Bulk and Surface Defects



Assessment of Proposed Physical Models

The zero level data analysis lessens the relevance of some physical models proposed to explain the field dependent surface resistance. If the penetration depth λ were field dependent, it is hard to see, why A ($\sim \lambda^3$), is proportional to R_{res} as in Fig. 1d). If the energy gap Δ were field dependent, it is equally hard to see, why the lines of the plot in Fig. 1.e) are parallel.

CONCLUSION

We presented the essential features, partly as a summary of previously published work, of a model

describing the field dependence of the Q-value (or, equivalently, the surface resistance) in sc bulk niobium accelerating cavities for the entire data range from 1.5 K to 4.25 K. We compared the model with recent data on so called “N-doping” of sc cavities. This model is based on the two-fluid description of the surface resistance and the postulated presence of weak sc defects. The model essentially uses a single parameter, the conductivities of the nc current components of the superconductor or, equivalently, their mean free paths, respectively. Other major features are the sc proximity effect, percolation behaviour, and the distinction between surface and bulk properties, the surface conditions being more determinant for the power dissipation than the bulk conditions. The necessary conditions, according to this model, for obtaining a very small surface resistance (in the nΩ range) and an increase of the Q-value with field by “N-doping” are these: (i) minimization of the number of superficial weak sc defects by, e.g. electro-polishing, and their diffusion into the bulk by, e.g. thermal annealing; (ii) growing of weak sc defects in the bulk with large N content with the aim to push the percolation (fragmentation) to a temperature above the envisaged operation temperature. Finally, the data put some doubt on several physical models for the field dependent surface resistance.

ACKNOWLEDGMENT

We thank Dan Gonnella for developing the data collection technique, collecting the Q data shown and making it available to us. We thank Georg Hoffstaetter for raising the question of how to combine resistivities that is a main concern of this paper, and thank Dan Gonnella, Georg Hoffstaetter, and Matthias Liepe for many useful discussions regarding contributions to the residual resistivity and to the combination of residual and BCS resistivities.

This work was supported by DOE grant DE-FG02-13ER42058/SC0010564 and NSF grant PHY-1002467.

REFERENCES

- [1] A. Grassellino et al., Supercond. Sci. Technol. 26 (2013) 102001.
- [2] G. Ciovati et al, Appl. Phys. Lett. **104**, 092601 (2014); <http://dx.doi.org/10.1063/1.4867339>.
- [3] Dan Gonnella et al., arXiv:1411.1659.
- [4] Data were provided by M. Liepe and D. Gonnella, cf. also R. Eichhorn et al., arXiv:1407.3220.
- [5] Cf. a review of proposed models by 2003: B. Visentin, 11th Workshop RF Superconductivity, Lübeck-Travemünde.
- [6] W. Weingarten, Phys. Rev. ST-AB **14** (2011) 101002.
- [7] Binping Xiao and Charles E. Reece, arXiv 1404:2523.
- [8] A. Gurevich, Physica **C 441** (2006) 38.
- [9] G. Linker, in W. Buckel, W. Werner, eds., Proceedings of the IV International Conference, *Superconductivity in d- and f-Band Metals*, Kernforschungszentrum Karlsruhe (Germany), 1982, p. 367.